Published in final edited form as:
Phys Med Biol. 2008 November 7; 53(21): 6055–6063. doi:10.1088/0031-9155/53/21/011.

An image acquisition and registration strategy for the fusion of hyperpolarized helium-3 MRI and x-ray CT images of the lung

Rob H Ireland[1,2], **Neil Woodhouse**[1], **Nigel Hoggard**[1], **James A Swinscoe**[2], **Bernadette H Foran**[2], **Matthew Q Hatton**[2], and **Jim M Wild**[1]

[1]Academic Unit of Radiology, University of Sheffield, Sheffield, UK

[2]Academic Unit of Clinical Oncology, University of Sheffield, Sheffield, UK

Abstract

The purpose of this ethics committee approved prospective study was to evaluate an image acquisition and registration protocol for hyperpolarized helium-3 magnetic resonance imaging (^{3}He-MRI) and x-ray computed tomography. Nine patients with non-small cell lung cancer (NSCLC) gave written informed consent to undergo a free-breathing CT, an inspiration breath-hold CT and a 3D ventilation ^{3}He-MRI in CT position using an elliptical birdcage radiofrequency (RF) body coil. ^{3}He-MRI to CT image fusion was performed using a rigid registration algorithm which was assessed by two observers using anatomical landmarks and a percentage volume overlap coefficient. Registration of ^{3}He-MRI to breath-hold CT was more accurate than to free-breathing CT; overlap 82.9 ± 4.2% versus 59.8 ± 9.0% ($p < 0.001$) and mean landmark error 0.75 ± 0.24 cm versus 1.25 ± 0.60 cm ($p = 0.002$). Image registration is significantly improved by using an imaging protocol that enables both ^{3}He-MRI and CT to be acquired with similar breath holds and body position through the use of a birdcage ^{3}He-MRI body RF coil and an inspiration breath-hold CT. Fusion of ^{3}He-MRI to CT may be useful for the assessment of patients with lung diseases.

1. Introduction

Over the last decade, the technology for magnetic resonance imaging (MRI) with inert gases such as hyperpolarized helium-3 (^{3}He) has emerged for lung ventilation imaging (Wild *et al* 2002) and has been clinically applied to diseases such as cystic fibrosis, asthma and emphysema (Donnelly *et al* 1999, Salerno *et al* 2002, van Beek *et al* 2004, Fain *et al* 2006). Hyperpolarized gas imaging enables novel quantitative analysis of pulmonary physiology (Wild *et al* 2004) and has the potential to provide clinical information superior to single-photon emission computed tomography (SPECT) without the need for radioisotopes (Stavngaard *et al* 2005).

As with other functional radiological investigations, there may be significant benefits in combining ^{3}He-MR images to the anatomical structure provided by x-ray computed tomography (CT) or ^{1}H-MRI (Woodhouse *et al* 2005). Accurate image registration is an essential requirement for such multimodality assessment of patients with lung disease. In this paper, we demonstrate an image acquisition and registration strategy for the fusion of ^{3}He-MRI and x-ray CT and discuss its potential application to lung cancer treatment planning and monitoring.

E-mail: r.ireland@sheffield.ac.uk.

Europe PMC Funders Author Manuscripts

Before radiotherapy treatment, many patients have ventilation or perfusion defects that impair effective lung function. The concept of functionally weighted treatment planning is to identify regions of defective lung and of viable functioning lung and to allow the radiotherapy inverse planning algorithm to apply different dose constraints to healthy and impaired lung tissue. This strategy has been applied using SPECT with the aim of reducing the incidence of treatment complications by modifying the dose distributions within the lung while maintaining tumour toxicity (Marks *et al* 1993, 1999, McGuire *et al* 2006, Lavrenkov *et al* 2007, Shioyama *et al* 2007).

For the information provided by ^{3}He-MRI to be used in radiotherapy in a similar manner to SPECT, the MR images need to be accurately registered to the lung CT scans that are routinely used for treatment planning. The only previous work related to such ^{3}He-MR image registration was a recently reported pilot study (Ireland *et al* 2007) in which the feasibility of acquiring ^{3}He-MRI for non-small cell lung cancer (NSCLC) patients was demonstrated. While the study showed that ^{3}He-MR images could be registered to radiotherapy CT for use in treatment planning, a number of changes to both the MR and CT protocol were identified that could enhance the registration accuracy. The key components required to make these changes have recently been realized. These include a new radiofrequency (RF) body coil, which has been designed, built and tested (de Zanche *et al* 2008), a 3D ^{3}He-MR volume imaging methodology (Wild *et al* 2004) and the use of a 16-slice radiotherapy CT scanner. These advances have enabled the implementation of treatment position ^{3}He-MR imaging and breath-hold planning CT. The aim of this study was to utilize the modified ^{3}He-MRI and CT acquisition protocols and quantify the impact of breath hold on the accuracy of ^{3}He-MRI to CT image registration.

2. Materials and methods

2.1. NSCLC patients

Patients with histologically confirmed NSCLC due to undergo CT for radiotherapy planning were recruited to the study by consultant oncologists. All patients gave written informed consent to participate, and the prospective study was approved by the Local Research Ethics Committee. Each patient underwent hyperpolarized ^{3}He-MRI in addition to two x-ray CTs.

2.2. MR image acquisition

Hyperpolarized ^{3}He-MR ventilation imaging was performed on a 1.5 T whole body Eclipse system (Philips Medical Systems, Cleveland, OH, USA), which was fitted with a second RF amplifier (2 kW, Analogic Corporation, Peabody, MA, USA) and a transmit–receive circuit tuned to 48.5 MHz for ^{3}He (Wild *et al* 2004).

In the previous work (Ireland *et al* 2007), patients were imaged with a twin saddle quadrature transmit–receive RF coil (IGC Medical Advances, Milwaukee, WI, USA), which required the patients to be imaged supine with their arms down. More recently, a volume coil has been developed (de Zanche *et al* 2008) that provides ^{3}He-MR images which can be acquired with the patients in treatment position (immobilized with their arms up). The coil design is an elliptical high pass birdcage that operates in quadrature mode. For ease of patient access, the coil splits into two halves and rests on the MR scanner patient bed. To mitigate interactions with the proton (^{1}H) RF body coil, the outer surface of the coil is screened. Tests on the coil indicate a higher B1 homogeneity and sensitivity in terms of image SNR; both are important considerations for high spatial resolution imaging of ^{3}He in the lungs (de Zanche *et al* 2008).

The birdcage coil was used with a 3D acquisition sequence (Wild *et al* 2004) that consists of a low flip angle ($\theta = 4°$), [96, 24] phase encodes in the [*y, z*] axes, 256 samples in the read

encoding direction [*x*], 9.33 mm slice thickness with no gap, FOV = 42.6 cm, TE = 3.25 ms, TR = 6 ms and bandwidth = 31.25 kHz. Each image was interpolated to 256 × 256 pixels with 1.66 mm pixel size. The ^{3}He gas (Spectra Gases, Huntingdon, UK) was polarized on site to approximately 30% by optical pumping with rubidium spin exchange apparatus (GE Healthcare, Princeton, NJ, USA). The investigators hold a license for ^{3}He gas polarization as an Investigational Medicinal Product from the national regulatory body. *In vivo* imaging was performed during a single 16 s breath hold of a 500 ml ^{3}He plus 500 ml N_2 mixture inhaled from a Tedlar bag (Jensen Inert Products, Coral Springs, FL, USA).

The ^{3}He gas was inhaled from a starting point of functional residual capacity and no additional inhalation of room air was permitted. Blood oxygen saturation was monitored via an MRI compatible pulse oximeter throughout the procedure. Patients were coached in the breathing manoeuvre and were allowed a trial breath hold with a dummy bag containing room air prior to imaging.

2.3. CT image acquisition

On the same day as ^{3}He-MR imaging, all patients underwent two transaxial CTs with a 16-slice Lightspeed CT (GE Healthcare, Princeton, NJ, USA). Initially, the patients were imaged in the conventional treatment planning position, which is supine with arms supported above the head while breathing freely. Subsequently, a second CT was acquired during a 530 ms inspiration breath hold performed with a 1 L Tedlar bag filled with room air that enabled simulation of the ^{3}He-MRI breathing manoeuvre. CT imaging (120 kVp) was performed at 512 × 512 pixels per slice with pixel size 0.9766 mm and 2.5 mm slice thickness.

2.4. Image registration

Using in-house Matlab (MathWorks Inc., Natick, MA, USA) DICOM editing software, distance measurement DICOM tags of the ^{3}He-MR images were scaled by a factor of 1.3 to compensate for the lower ^{3}He gyromagnetic ratio than that of ^{1}H, and the Scanning Sequence tag (0018,0020) was modified to ‘EP’ to enable the ^{3}He-MR images to be imported into the Eclipse treatment planning system (Varian Medical Systems, Palo Alto, CA, USA).

Once imported, the rigid control point (Zitová and Flusser 2003) registration tool implemented in Varian Eclipse was used to register the ^{3}He-MRI to the planning CT. A median of 6 (range 4-7) anatomical landmarks (‘control points’) were used and the mean and maximum error of landmark accuracy were calculated. The registration was performed by two independent observers (both experienced consultant oncologists) who identified landmarks around the lung apex, mediastinum, main and segmental carina and the lung bases. Lung volumes including the trachea were automatically segmented from the CT using standard threshold levels. The ^{3}He-MRI was segmented from the noise using a threshold set at three times the standard deviation of the background noise. In addition to anatomical landmarks, registration accuracy was quantified using an overlap coefficient (Ω), which is calculated as the proportion of the segmented ^{3}He-MR slice volume (V_{MRI}) that intersects the segmented CT lung slice volume (V_{CT}) expressed as a percentage of V_{MRI}:

$$\Omega = 100 \times \frac{V_{\mathrm{MRI}} \cap V_{\mathrm{CT}}}{V_{\mathrm{MRI}}}$$

where the higher the overlap value the better the registration. Values for the overlap are calculated from the entire MR and CT lung volumes.

As the ^{3}He-MR ventilated volume may be different than the CT defined volume due to the possibility of ventilation defects detected in the functional images, the overlap coefficient is a more appropriate measure of ^{3}He-MR to CT registration accuracy rather than, for example, the intersection-union ratio, which might have been used if the two volumes were expected to be similar.

After an interval of 3 months, the observers repeated the registration procedure and both inter- and intra-observer variability were assessed.

2.4.1. Effect of image resolution—The ^{3}He-MRI is acquired at a lower resolution than the planning CT. Once registered, within the treatment planning system the MRI is displayed overlaid with the planning CT. To evaluate the limit on image registration accuracy that results from the mismatch in image resolution alone, a low-resolution inspiration planning CT was created in Matlab using cubic decimation to the dimensions of the ^{3}He-MRI. The low-resolution CT was imported back into the treatment planning system and registered to the original high-resolution image volume. CT lung volumes were automatically segmented for both low- and high-resolution image sets. An overlap coefficient was then calculated from the low- and high-resolution lung volumes. This procedure was conducted for all of the nine patients to provide a theoretical limit of overlap performance taking into account the differing image resolution.

2.5. Statistical analysis

To test the statistical significance of differences between the registration accuracy of ^{3}He-MRI to conventional and breath-hold planning CT, analysis of variance tests were used with the mean error, maximum error and overlap coefficient as a dependent variable, the observers and CT type (free breathing and breath hold) as fixed factors and the subjects as a random factor.

Inter-observer variability was evaluated using analysis of variance applied to each parameter and CT type, with the observers as a fixed factor and the subjects as a random factor. Intra-observer variability was evaluated using one way analysis of variance applied to each parameter and CT type, with the subjects as a random factor. The Bland and Altman repeatability coefficient was used to summarize the inter- and intra-observer agreements (Bland and Altman 1999).

Statistical analysis was performed using SPSS for Windows (SPSS Version 15.0; Chicago, IL, USA). A p value of less than 0.05 was considered statistically significant. Data normality was verified with the Kolmogorov-Smirnov test. Bland–Altman plots were used to check the independence of the mean and difference values between observers for each parameter to ensure that a logarithmic transformation was not required (Bland and Altman 1999).

3. Results

3.1. NSCLC patients

Between April 2006 and March 2007, ten NSCLC patients underwent ^{3}He-MRI and CT with the new imaging equipment and protocol. There were 7 men and 3 women with mean age 71 years and age range 56-85 years. None of the patients had been previously treated with radiotherapy of the thorax. Patients had WHO performance status of 0-2 and forced expiratory volume (FEV1) > 1.5 L. During ^{3}He-MR imaging, no clinically significant decrease in blood oxygen saturation was observed and no ill effects were reported following inhalation of the ^{3}He/N_2 gas mixture. Due to a poor intake of gas, the ^{3}He-MRI for one

patient failed to produce ventilation images of sufficient quality for further registration analysis; therefore, nine MR scans were available for evaluation.

3.2. Image registration

3.2.1. ^{3}He-MR and planning CT—Calculated from the mean values for the two observers, the ^{3}He-MRI and conventional planning CT were registered with an overlap (mean ± SD) 59.8 ± 9.0%, mean landmark error 1.25 ± 0.60 cm and maximum landmark error 2.04 ± 1.06 cm (table 1). For the breath-hold CT, the overlap was 82.9 ± 4.2% ($p < 0.001$), mean landmark error 0.75 ± 0.24 cm ($p = 0.002$) and maximum landmark error 1.20 ± 0.36 cm ($p = 0.004$), which are all significantly better than for the registration of ^{3}He-MRI to conventional CT.

Example ^{3}He-MR images registered to conventional free-breathing CT and breath-hold CT are shown for two patients in figure 1.

The intra-observer and inter-observer variability are summarized in table 2. The analysis of variance for inter-observer variability demonstrated no significant difference between the two observers for each dependent variable or CT type ($p \geq 0.38$ for mean error, maximum error and overlap coefficient). There was no consistent pattern for inter-and intra-observer repeatability coefficient, as four values were smaller in the breath-hold case and five for the free-breathing data.

3.2.2. Effect of image resolution—A pseudo-planning CT was used to calculate a maximum limit of overlap taking into account the difference in image resolution between the original MR and CTs. Low-resolution CT was registered and overlaid with its original high-resolution version to give a mean error of 0.28 ± 0.10 cm, of maximum error of 0.49 ± 0.21 cm and an overlap value 96.2 ± 2.0%. Dividing the mean overlap for ^{3}He-MRI by this value provides a normalized overlap for the image resolution of 86.2% for the inspiration CT and 62.2% for the free-breathing CT.

4. Discussion

4.1. Image registration

Related studies have investigated the optimal acquisition protocol for SPECT and CT (Gutman *et al* 2005, Utsunomiya *et al* 2005, Suga *et al* 2007), and image registration of perfusion MRI and ^{3}He-MRI using controlled gas administration in pigs (Hong *et al* 2005, Rizi *et al* 2003). However, our work is the first to consider optimizing an image acquisition protocol for image registration of *in vivo* ^{3}He-MRI to CT.

Previously, patients have been imaged with a twin saddle coil for MR imaging and a single-slice scanner for CT (Ireland *et al* 2007). However, as the tight-fitting coil jacket impeded arm movement, ^{3}He-MRI with the original coil required imaging to be performed with arms down by the side of the patient during a breath hold of 1L of gas. This is a different imaging setup than is commonly used for conventional treatment planning which requires a free-breathing CT with the patient immobilized with their arms up behind the head. In addition, free-breathing treatment planning CT often contains artefacts at the base of the lung. These differences in patient positioning and image acquisition inevitably lead to errors in image registration when a rigid algorithm is applied.

Rather than using nonrigid image registration, which is difficult to apply and validate for the chest (Gutman *et al* 2005), lung image registration can be improved by using an imaging strategy that minimizes the differences in breathing protocol and body position between the MR and CT acquisitions. Consistent arm position was provided by an elliptical birdcage ^{3}He

body RF coil (de Zanche *et al* 2008) that made it possible to acquire higher quality ^{3}He-MR images using a 3D volume sequence (Wild *et al* 2004) in treatment position, and the installation of a 16-slice CT scanner that enabled a breath-hold CT to be acquired within a 5 s interval. This acquisition protocol enabled the thoracic image registration to be performed accurately with commercially available rigid registration software.

The statistical analysis outlined in section 3.2.1 demonstrates that the repeatability of image registration of ^{3}He-MRI to breath-hold CT and free-breathing CT is similar. For each parameter of registration accuracy (table 1), analysis of variance provides p values less than 0.004, 95% confidence intervals that do not contain zero and effect sizes that are large. Therefore, it is reasonable to conclude that there is a statistically and clinically significant difference in ^{3}He-MRI registration accuracy between the free-breathing and breath-hold CT.

4.2. Treatment planning

Image registration is an essential step towards implementing functionally weighted radiotherapy treatment planning. The potential for modifying lung cancer treatment plans with functional information has been investigated for SPECT (Marks *et al* 1993, 1999, McGuire *et al* 2006, Lavrenkov *et al* 2007, Shioyama *et al* 2007), 4D-CT (Yaremko *et al* 2007) and ^{3}He-MRI (Ireland *et al* 2007). Although free-breathing CT has been the most commonly used method of planning lung radiotherapy treatment, there may be benefits from using breath-hold techniques (Keall *et al* 2006, Duggan *et al* 2007, Nakamura *et al* 2007). Image registration provided by the breath-hold image acquisition protocol evaluated here could be beneficial in the implementation of ^{3}He-MRI-influenced treatment planning. Similarly, registration of ^{3}He-MRI and CT could be useful for comparing pre- and post-treatment images for treatment monitoring and long-term follow-up.

4.3. Other applications

As demonstrated in other areas of radiology such as SPECT/CT (Suga *et al* 2007), accurate fusion of anatomical and functional data can assist image interpretation. Although the current study has focused on the application of ^{3}He-MRI to lung cancer patients, MR ventilation imaging is more established in the study of other lung diseases (van Beek *et al* 2004). In such cases, registration of ^{3}He-MRI to CT would enable pulmonary ventilation to be assessed against the underlying anatomical CT structure which serves as the gold standard. Potential applications include the analysis of serial studies conducted with ^{3}He-MRI. When the reduction of radiation dose is important, it may also be appropriate to assess lung disease with ^{3}He-MRI in conjunction with anatomical images provided by ^{1}H-MRI rather than CT. For example, an approach similar to that described in this work could also be applied to the registration of ^{3}He-MRI to ^{1}H-MRI with the aim of further improving quantification accuracy of the ratio of ventilated to total lung volume (Woodhouse *et al* 2005).

Furthermore, if ^{3}He-MRI is to become a complementary or superior lung imaging technique in a clinical setting, then quantitative metrics of its performance are needed to allow comparison against existing imaging modalities (McMahon *et al* 2006). These quantitative comparisons will require accurate spatial registration.

4.4. Limitations

One limitation with matching ^{3}He-MRI to CT is the difference in image resolution. The impact of this on image registration can be estimated from constructing pseudo-CT data sets at the resolution of the MRI. Reproducibility of patient breath hold is another limiting factor that requires further investigation for ^{3}He-MRI though reproducibility of breath-hold CT has

been shown to be feasible for selected groups of NSCLC patients (Keall *et al* 2006, Duggan *et al* 2007, Nakamura *et al* 2007).

5. Conclusions

This study has demonstrated a method of registering hyperpolarized ^{3}He-MRI to x-ray CT. Compared with free-breathing CT, application of an inspiration CT acquired at a breath hold similar to that used in the MRI provides a statistically significant improvement of ^{3}He-MRI to CT image registration accuracy as measured by anatomical landmarks and an overlap coefficient.

Acknowledgments

Rob Ireland is funded by a Postdoctoral Award from the National Institute of Health Research (UK Department of Health: N&AHP/PDA/04/012). The UK EPSRC (grants GR/S81834/01P and EP/D070252/1), Yorkshire Cancer Research, Weston Park Hospital Cancer Appeal and Sheffield Hospitals Charitable Trust provided additional funding. We also thank Gillian Brown, Jan Johnson and Helen Simpson for their assistance and are grateful for the loan of the ^{3}He gas polarizer from GE Healthcare and support from Spectra Gases and Philips Medical Systems. Statistical advice was provided by a consultant Statistician within Statistical Services Unit, The University of Sheffield.

References

Bland JM, Altman DG. Measuring agreement in method comparison studies. Stat. Methods Med. Res. 1999; 8:135–60. [PubMed: 10501650]

de Zanche N, Chhina N, Teh K, Randell C, Pruessmann KP, Wild JM. Asymmetric quadrature split birdcage coil for hyperpolarized ^{3}He lung MRI at 1.5 T. Magn. Reson. Med. 2008; 60:431–8. [PubMed: 18666111]

Donnelly LF, MacFall JR, McAdams HP, Majure JM, Smith J, Frush DP, Bogonad P, Charles HC, Ravin CE. Cystic fibrosis: combined hyperpolarized 3He-enhanced and conventional proton MR imaging in the lung—preliminary observations. Radiology. 1999; 212:885–9. [PubMed: 10478261]

Duggan DM, Ding GX, Coffey CW II, Kirby W, Hallahan DE, Malcolm A, Lu B. Deep-inspiration breath-hold kilovoltage cone-beam CT for setup of stereotactic body radiation therapy for lung tumors: initial experience. Lung Cancer. 2007; 56:77–88. [PubMed: 17169461]

Fain SB, Panth SR, Evans MD, Wentland AL, Holmes JH, Korosec FR, O'Brien MJ, Fountaine H, Grist TM. Early emphysematous changes in asymptomatic smokers: detection with ^{3}He MR imaging. Radiology. 2006; 239:875–83. [PubMed: 16714465]

Gutman F, Hangard G, Gardin I, Varmenot N, Pattyn J, Clement JF, Dubray B, Véra P. Evaluation of a rigid registration method of lung perfusion SPECT and thoracic CT. Am. J. Roentgenol. 2005; 185:1516–24. [PubMed: 16304006]

Hong C, Leawoods JC, Yablonskiy DA, Leyendecker JR, Bae KT, Pilgram TK, Woodard PK, Conradi MS, Zheng J. Feasibility of combining MR perfusion, angiography, and ^{3}He ventilation imaging for evaluation of lung function in a porcine model. Acad. Radiol. 2005; 12:202–9. [PubMed: 15721597]

Ireland RH, Bragg CM, McJury M, Woodhouse N, Fichele S, van Beek EJ, Wild JM, Hatton MQ. Feasibility of image registration and intensity-modulated radiotherapy planning with hyperpolarized helium-3 magnetic resonance imaging for non-small-cell lung cancer. Int. J. Radiat. Oncol. Biol. Phys. 2007; 68:273–81. [PubMed: 17448880]

Keall PJ, et al. The management of respiratory motion in radiation oncology report of AAPM Task Group 76. Med. Phys. 2006; 33:3874–900. [PubMed: 17089851]

Lavrenkov K, Christian JA, Partridge M, Niotsikou E, Cook G, Parker M, Bedford JL, Brada M. A potential to reduce pulmonary toxicity: the use of perfusion SPECT with IMRT for functional lung avoidance in radiotherapy of non-small cell lung cancer. Radiother. Oncol. 2007; 83:156–62. [PubMed: 17493699]

Europe PMC Funders Author Manuscripts

Marks LB, et al. The utility of SPECT lung perfusion scans in minimizing and assessing the physiologic consequences of thoracic irradiation. Int. J. Radiat. Oncol. Biol. Phys. 1993; 26:659–68. [PubMed: 8330998]

Marks LB, Sherouse GW, Munley MT, Bentel GC, Spencer DP. Incorporation of functional status into dose-volume analysis. Med. Phys. 1999; 26:196–9. [PubMed: 10076973]

McGuire SM, Zhou S, Marks LB, Dewhirst M, Yin FF, Das SK. A methodology for using SPECT to reduce intensity-modulated radiation therapy (IMRT) dose to functioning lung. Int. J. Radiat. Oncol. Biol. Phys. 2006; 66:1543–52. [PubMed: 17126212]

McMahon CJ, Dodd JD, Hill C, Woodhouse N, Wild JM, Fichele S, Gallagher CG, Skehan SJ, van Beek EJ, Masterson JB. Hyperpolarized ^{3}helium magnetic resonance ventilation imaging of the lung in cystic fibrosis: comparison with high resolution CT and spirometry. Eur. Radiol. 2006; 16:2483–90. [PubMed: 16871384]

Nakamura K, Shioyama Y, Nomoto S, Ohga S, Toba T, Yoshitake T, Anai S, Terashima H, Honda H. Reproducibility of the abdominal and chest wall position by voluntary breath-hold technique using a laser-based monitoring and visual feedback system. Int. J. Radiat. Oncol. Biol. Phys. 2007; 68:267–72. [PubMed: 17448879]

Rizi RR, Saha PK, Wang B, Ferrante MA, Lipson D, Baumgardner J, Roberts DA. Co-registration of acquired MR ventilation and perfusion images—validation in a porcine model. Magn. Reson. Med. 2003; 49:13–8. [PubMed: 12509815]

Salerno M, de Lange EE, Altes TA, Truwit JD, Brookeman JR, Mugler JP III. Emphysema: hyperpolarized helium 3 diffusion MR imaging of the lungs compared with spirometric indexes—initial experience. Radiology. 2002; 222:252–60. [PubMed: 11756734]

Shioyama Y, et al. Preserving functional lung using perfusion imaging and intensity-modulated radiation therapy for advanced-stage non-small cell lung cancer. Int. J. Radiat. Oncol. Biol. Phys. 2007; 68:1349–58. [PubMed: 17446001]

Stavngaard T, Sogaard LV, Mortensen J, Hanson LG, Schmiedeskamp J, Berthelsen AK, Dirksen A. Hyperpolarised ^{3}He MRI and ^{81m}Kr SPECT in chronic obstructive pulmonary disease. Eur. J. Nucl. Med. Mol. Imaging. 2005; 32:448–57. [PubMed: 15821964]

Suga K, Kawakami Y, Iwanaga H, Tokuda O, Matsunaga N. Automated breath-hold perfusion SPECT/CT fusion images of the lungs. Am. J. Roentgenol. 2007; 189:455–63. [PubMed: 17646474]

Utsunomiya D, Nakaura T, Honda T, Shiraishi S, Tomiguchi S, Kawanaka K, Morishita S, Awai K, Ogawa H, Yamashita Y. Object-specific attenuation correction at SPECT/CT in thorax: optimization of respiratory protocol for image registration. Radiology. 2005; 237:662–9. [PubMed: 16170014]

van Beek EJ, Wild JM, Kauczor HU, Schreiber W, Mugler JP III, de Lange EE. Functional MRI of the lung using hyperpolarized 3-helium gas. J. Magn. Reson. Imaging. 2004; 20:540–54. [PubMed: 15390146]

Wild JM, et al. MR imaging of the lungs with hyperpolarized helium-3 gas transported by air. Phys. Med. Biol. 2002; 47:N185–90. [PubMed: 12164592]

Wild JM, Woodhouse N, Paley MN, Fichele S, Said Z, Kasuboski L, van Beek EJ. Comparison between 2D and 3D gradient-echo sequences for MRI of human lung ventilation with hyperpolarized ^{3}He. Magn. Reson. Med. 2004; 52:673–8. [PubMed: 15334590]

Woodhouse N, Wild JM, Paley MN, Fichele S, Said Z, Swift AJ, van Beek EJ. Combined helium-3/proton magnetic resonance imaging measurement of ventilated lung volumes in smokers compared to never-smokers. J. Magn. Reson. Imaging. 2005; 21:365–9. [PubMed: 15779032]

Yaremko BP, Guerrero TM, Noyola-Martinez J, Guerra R, Lege DG, Nguyen LT, Balter PA, Cox JD, Komaki R. Reduction of normal lung irradiation in locally advanced non-small-cell lung cancer patients using ventilation images for functional avoidance. Int. J. Radiat. Oncol. Biol. Phys. 2007; 68:562–71. [PubMed: 17398028]

Zitová B, Flusser J. Image registration methods: a survey. Image Vis. Comput. 2003; 21:977–1000.

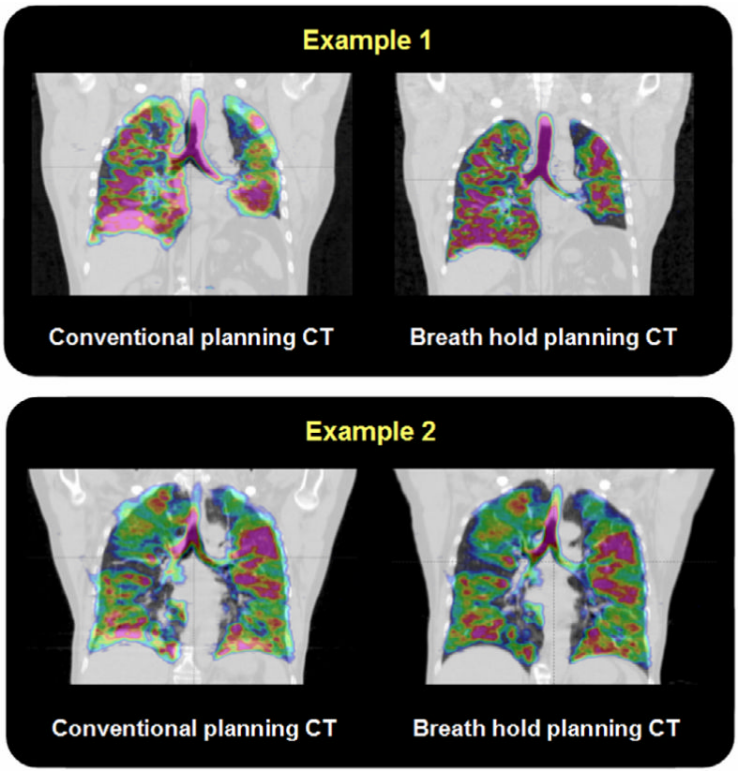

Figure 1.
Two examples of registered coronal hyperpolarized ^{3}He-MRI (colour) displayed fused with radiotherapy treatment planning conventional, free-breathing CT (left) and inspiration breath-hold CT (right).

Europe PMC Funders Author Manuscripts

Europe PMC Funders Author Manuscripts

Table 1

Comparison of registration accuracy results (mean ± SD) for ^{3}He-MRI to free-breathing CT and breath-hold CT

	^{3}He to free-breathing CT	^{3}He to breath-hold CT	*p* value	95% confidence interval for mean difference	Effect size (mean difference)
Mean landmark error	1.25 ± 0.60 cm	0.75 ± 0.24 cm	$p = 0.002$	−0.81 to −0.20 cm	−0.50 cm
Max landmark error	2.04 ± 1.06 cm	1.20 ± 0.36 cm	$p = 0.004$	−1.34 to −0.30 cm	−0.84 cm
Overlap	59.8 ± 9.0%	82.9 ± 4.2%	$p < 0.001$	18.3 to 27.9%	23.1%

Phys Med Biol. Author manuscript; available in PMC 2009 July 22.

Europe PMC Funders Author Manuscripts

Table 2

Repeatability coefficients for inter- and intra-observer variability

	Breath-hold CT			Free-breathing CT		
	Mean	**Max**	**Overlap**	**Mean**	**Max**	**Overlap**
Intra-observer 1	0.90 cm	1.65 cm	4.9%	1.76 cm	2.91 cm	4.0%
Intra-observer 2	0.87 cm	1.09 cm	5.7%	0.70 cm	1.73 cm	1.6%
Inter-observer	0.33 cm	0.92 cm	1.4%	0.97 cm	0 cm	0.9%